JACS
JOURNAL OF THE AMERICAN CHEMICAL SOCIETY
Communication
pubs.acs.org/JACS

Transformation of Pd Nanocubes into Octahedra with Controlled Sizes by Maneuvering the Rates of Etching and Regrowth

Maochang Liu,[†,‡] Yiqun Zheng,[§] Lei Zhang,[†] Liejin Guo,[‡] and Younan Xia*[,†,§]

[†]The Wallace H. Coulter Department of Biomedical Engineering, Georgia Institute of Technology and Emory University, Atlanta, Georgia 30332, United States

[‡]International Research Center for Renewable Energy, State Key Laboratory of Multiphase Flow, Xi'an Jiaotong University, Xi'an, Shaanxi 710049, P. R. China

[§]School of Chemistry and Biochemistry, School of Chemical and Biomolecular Engineering, Georgia Institute of Technology, Atlanta, Georgia 30332, United States

Supporting Information

ABSTRACT: Palladium octahedra with controlled edge lengths were obtained from Pd cubes of a single size. The success of this synthesis relies on a transformation involving oxidative etching and regrowth. Because the {100} side faces of the Pd nanocubes were capped by Br^- ions, Pd atoms were removed from the corners during oxidative etching, and the resultant Pd^{2+} ions could be reduced and deposited back onto the nanocubes, but preferentially on the {100} facets. We could control the ratio of the etching and regrowth rates ($R_{etching}$ and $R_{regrowth}$) simply by varying the amount of HCl added to the reaction solution. With a large amount of HCl, etching dominated the process ($R_{etching} \gg R_{regrowth}$), resulting in the formation of Pd octahedra with an edge length equal to 70% of that of the cubes. In contrast, with a small amount of HCl, all of the newly formed Pd^{2+} ions could be quickly reduced and deposited back onto the Pd cubes. In this case, $R_{etching} \approx R_{regrowth}$, and the resultant Pd octahedra had roughly the same volume as the starting cubes, together with an edge length equal to 130% of that of the cubes. When the amount of HCl was between these two extremes, we obtained Pd octahedra with intermediate edge lengths. This work not only advances our understanding of oxidative etching in nanocrystal synthesis but also offers a powerful means for controlling the shape and size of metal nanocrystals simply by adjusting the rates of etching and regrowth.

Shape-controlled synthesis of noble-metal nanocrystals has received increasing attention because of their attractive and tunable properties that are beneficial to many applications in catalysis, electronics, photonics, sensing, and biomedical research.[1] Thanks to the efforts of many groups, it is now possible to generate noble-metal nanocrystals with a wide variety of shapes, including cubes, octahedra, tetrahedra, decahedra, icosahedra, bars, wires, plates, and bipyramids, and most of their growth mechanisms have also been elucidated.[1j,2]

Seed-mediated growth has recently emerged a simple, robust, and powerful route for the synthesis of nanocrystals with both simple and complex shapes.[3] When nanocrystals with well-defined shapes (typically, cubes and octahedra) are used as the seeds, it is possible to track the growth pathway and thus decipher the mechanistic details, including the deposition and surface diffusion of atoms during a growth process.[4] Despite significant progress in recent years, many issues still remain unsolved. In the growth of cubic seeds, as an example, one can only obtain octahedra of a single size, which is roughly 2.1 times of the edge length of the cubic seed.[5] After reaching this point, the growth is automatically terminated, and this self-termination makes it very inconvenient to generate octahedra with different sizes. In general, cubic seeds of different sizes have to be used.

In addition to seeded growth, oxidative etching of preformed nanocrystals offers another versatile route to new shapes or morphologies. Typically, oxidative etching can occur in the presence of O_2 from air and a proper coordination ligand for the metal ions (e.g., Cl^- or Br^-), by which zero-valent metal atoms can be oxidized into the ionic form.[1j,6] We have demonstrated that nanocrystals with defects such as twinning or stacking faults are more susceptible to oxidative etching than their single-crystal counterparts.[6a,7] By taking advantage of this selectivity, we were able to selectively remove twinned seeds (or nanocrystals) from a reaction solution so that the final product was dominated by single-crystal species. We also found that Br^- was less corrosive than Cl^-. Simply replacing Cl^- with Br^- enabled the elimination of only the multiple-twinned seeds while allowing single-twinned seeds to evolve into right bipyramids.[7a,b] In another work, we further demonstrated that Fe^{3+}/Br^- pairs can serve as a much stronger etchant to attack and dissolve single-crystal nanoparticles made of Pd.[4b]

In spite of these successful demonstrations, it remains a grand challenge to use oxidative etching in a more controllable way to maneuver the size, shape, and morphology of metal nanocrystals, especially for single-crystal structures. There are a few reports on the use of oxidative etching to transform Ag cubes or octahedra into spheres, multipods, and asymmetric structures.[2e,8] Most of these studies involved nanocrystals of large sizes (typically >40 nm), and none of them took into consideration a possible regrowth process when the resultant metal ions were subsequently reduced. In fact, the fate (e.g., redeposition) of the ions generated from dissolution of the original seeds could

Received: June 23, 2013
Published: July 31, 2013

dx.doi.org/10.1021/ja406344j | J. Am. Chem. Soc. 2013, 135, 11752−11755

play a key role in determining the shape of resultant nanocrystals.[9] Here we demonstrate that Pd nanocubes of one size can be transformed into Pd octahedra with a range of controlled sizes without the addition of more Pd precursor simply by manipulating the rate of oxidative etching relative to the rate of regrowth.

Figure 1 shows a schematic of the oxidative etching and regrowth process that leads to the transformation of Pd

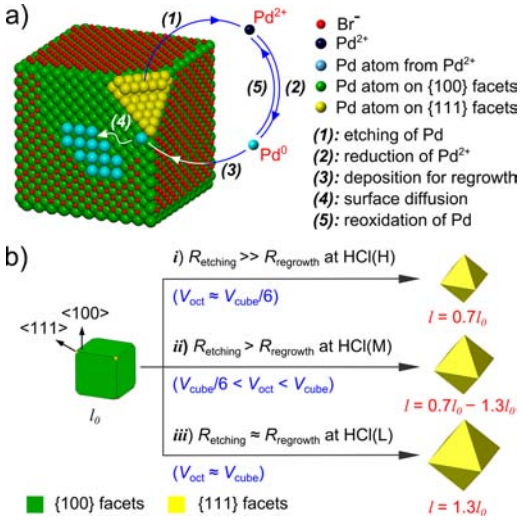

Figure 1. (a) Schematic illustration of the five major steps involved in the oxidative etching and regrowth process. Because all of the the side faces of the Pd cube are capped by Br^- ions, Pd atoms are mainly etched from the corner site(s), and the resultant Pd^{2+} ions can be subsequently reduced and deposited onto the side faces. (b) Schematic illustrations showing the formation of Pd octahedra with different but controllable edge lengths (l) by maneuvering the rates of oxidative etching and regrowth for Pd cubes with an edge length of l_0 HCl at different concentrations from high (H) to low (L).

nanocubes into octahedra with controlled sizes. Each Pd nanocube is enclosed by six {100} facets, all of which are passivated by a monolayer of chemisorbed Br^- ions.[10] The use of starting nanocrystals with a well-defined shape and the blocking of {100} facets by Br^- ions allowed us to easily track the etching process in a precise way by analyzing the shapes of products obtained at different stages of the reaction. Figure 1a illustrates the five major steps involved in the transformation process. Because of the passivation of all of the side faces by Br^- ions and the high energy associated with corner sites, oxidative etching and removal of the Pd atoms should start at the corners and proceed in the ⟨111⟩ directions (step 1). These newly generated Pd^{2+} ions can be reduced back to the elemental form, Pd atoms, when there is a reductant in the solution (step 2). These Pd atoms are then deposited onto the edges because of the edges' high energy and the unavailability of corner sites (step 3). The atoms can further diffuse to the adjacent side faces (step 4). The involvement of surface diffusion in nanocrystal growth was systematically investigated in our recent work.[4a] It should be pointed out that the Pd atoms generated by reduction (step 2) can also be oxidized back to Pd^{2+} again in a strongly corrosive environment (step 5). In this case, the volume of the resultant nanocrystal is smaller than that of the original nanocube. Since the etching occurs at corners along the ⟨111⟩ directions, the final product is a Pd octahedron because the {111} facets have the lowest surface free energy in the absence of a capping agent for the {100} facets.[6b,11] The concentration of the Br^- ions released from the nanocubes during etching is inadequate for them to serve as a capping agent for the {100} facets. Figure S1a in the Supporting Information shows the relationships between a cube and the resultant octahedra, including the smallest octahedron that could be obtained by etching of a nanocube ($V_{oct} \approx V_{cube}/6$) as well as the largest octahedron that could be obtained by preserving the volume ($V_{oct} \approx V_{cube}$). More significantly, controlling the oxidative etching rate ($R_{etching}$) relative to the regrowth rate ($R_{regrowth}$) allowed the size of the resultant octahedra to be controlled between these two extremes.

Our experiments were carried out with HCl/O_2 as the oxidative etchant and triethylene glycol (Tri-EG) as the reducing agent. We could easily adjust $R_{etching}$ relative to $R_{regrowth}$ by simply adjusting the concentration of HCl. At a high concentration, the Pd atoms formed by reduction of etched Pd^{2+} (step 2) are reoxidized (step 5) before they can be deposited back onto the surface of the cube (step 3). In other words, steps 3 and 4 in Figure 1a are greatly suppressed because of the significant acceleration of step 5. In this case, regrowth is negligible relative to etching ($R_{etching} \gg R_{regrowth}$), resulting in the formation of a Pd octahedron with the shortest edge length (condition *i* in Figure 1b). For a Pd nanocube with an edge length of l_0, the smallest octahedron should have an edge length (l) of $0.7l_0$ (Figure S1a). On the contrary, when the concentration of HCl is low, all of the atoms etched from the corners are reduced and redeposited back onto the cube. As a result, the total volume of the octahedron is the same as that of the initial cube (situation *iii* in Figure 1b), and the edge length of the octahedron is $1.3l_0$ (Figure S1a). A similar argument can be applied to intermediate cases, where a portion of the newly generated Pd atoms are reoxidized back to Pd^{2+} ions before they are deposited onto the initial seed. The volume of the resultant octahedron in such cases is therefore between the above two extremes ($V_{cube}/6 < V_{oct} < V_{cube}$; situation *ii* in Figure 1b).

We carried out a series of experiments according to the above rationales. In brief, we mixed a suspension of Pd cubes (serving as the sacrificial templates for etching and the seeds for regrowth) with poly(vinylpyrrolidone) as a stabilizer in Tri-EG (8 mL) as both the solvent and reductant, and HCl/O_2 was added as the etchant for elemental Pd. The two rates, $R_{regrowth}$ and $R_{etching}$, were controlled simply by adjusting the HCl concentration. Figure 2

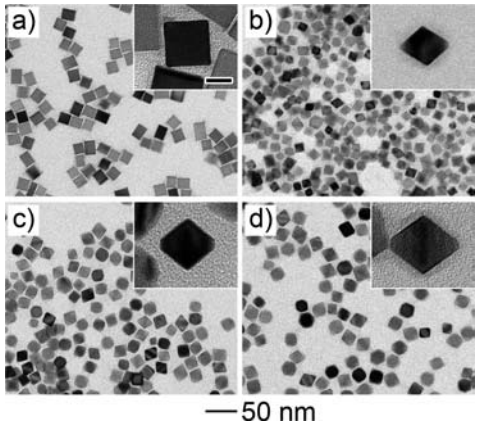

Figure 2. TEM images of (a) Pd nanocubes with an edge length of 18 nm and (b–d) Pd octahedra with edge lengths of 13, 18, and 23 nm prepared by etching with the addition of 180, 120, and 60 μmol of HCl, respectively. The scale bar in the inset of (a) is 10 nm and applies to the other insets also. The scale bar of 50 nm applies to all of the images.

dx.doi.org/10.1021/ja406344j | J. Am. Chem. Soc. 2013, 135, 11752–11755

shows transmission electron microscopy (TEM) images of Pd nanocubes and the as-prepared octahedra. The Br^--capped nanocubes were prepared according to our previous report[12] and had an average edge length of l_0 = 18 nm (Figure 2a). Closer examination indicated that some of the nanocubes were in fact nanobars with a slight elongation along one of the axes; these were also covered by six Br^--capped {100} facets. To simplify our discussion, the nanocubes and nanobars are collectively called "nanocubes". As shown in Figure S1b, the final product from a bar with an aspect ratio slightly larger than 1 is also an octahedron. Figure 2b–d shows TEM images of the size-controlled octahedra synthesized by adding 180, 120, or 60 μmol of HCl, respectively, into the reaction solution. By careful measurement of their projected edge lengths viewed along the [110] direction, the average edge lengths of these octahedra were determined to be 13.4 ± 3.4, 18.4 ± 2.7, and 22.6 ± 3.1 nm, respectively (Figure S2). In view of the relationship between the edge lengths of a nanocube and the resultant octahedron, the ratios of the edge lengths were calculated to be about 0.7, 1, and 1.3, which matched well with our predicted ratios shown in Figure 1b, validating the mechanism illustrated in Figure 1a. In particular, with 180 μmol of HCl, the Pd atoms were quickly oxidized back to Pd^{2+} ions, resulting in $R_{regrowth} \approx 0$ and thereby the formation of the smallest octahedra. In contrast, with 60 μmol of HCl, all of the Pd atoms were essentially deposited back onto the original cubes, leading to the formation of the largest octahedra. The use of HCl at an intermediate concentration resulted in Pd octahedra with a size between these two extremes.

To better understand the oxidative etching and regrowth process, we further checked the shape evolution at different stages of a synthesis. We only focused on the extreme cases shown in Figure 2b,d, which involved the addition of 180 and 60 μmol of HCl, respectively, as the etchant. Clearly, with the use of a large amount of HCl, the nanocubes were quickly transformed into cuboctahedra (Figure 3a, t = 0.5 h) and truncated

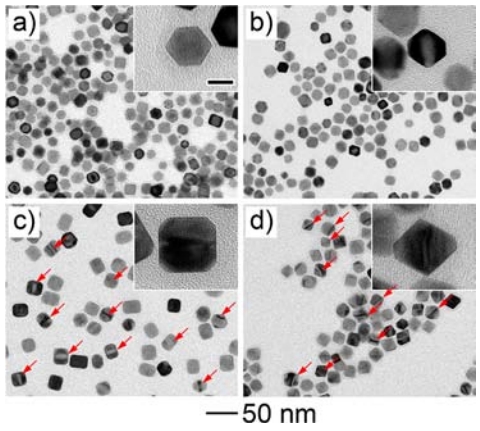

Figure 3. TEM images of Pd nanocrystals obtained at different stages of the etching process with the addition of (a, b) 180 and (c, d) 60 μmol of HCl. The etching times were (a, c) 0.5 h and (b, d) 1 h. The scale bar in the inset of (a) is 10 nm and applies to the other insets also. The red arrows indicate the unique strips generated during surface diffusion.

octahedrons (Figure 3b, t = 1 h). In the least corrosive environment, we obtained truncated cubes (Figure 3c, t = 0.5 h) and truncated octahedrons (Figure 3d, t = 1 h). These images clearly demonstrate the involvement of oxidative etching. In addition, some unique strips were also observed on the nanocrystals, as indicated by red arrows in Figure 3c,d. In fact, as shown in Figure 1a, the regrowth consisted of two steps: (*i*) deposition onto the high-energy edges (Figure 1a, step 3) and (*ii*) surface diffusion to the Br^--capped {100} facets (Figure 1a, step 4). The strips observed on the nanocrystals thus provided evidence to support the involvement of surface diffusion, as we recently discovered in another study.[4a] Nevertheless, the disappearance of such strips from the final product shown in Figure 2d implies that diffusion could occur throughout the reaction and would stop as soon as a flat surface was reached.

The oxidative etching and regrowth process could also be extended to smaller nanocubes with the formation of smaller octahedra. With 13 nm Pd nanocubes (Figure S3a), we obtained truncated Pd nanocubes (Figure S3b), and then octahedra with an edge length of 16 nm (Figure S3c) when 60 μmol of HCl was added to the reaction solution. As expected, the use of 180 μmol of HCl led to the formation of 9 nm octahedra (Figure S3d). Furthermore, we found that the reaction was very sensitive to the reaction temperature. Figure S4 shows TEM images of the products obtained from 18 nm nanocubes at 120 and 140 °C in the presence of 60 μmol of HCl for 2 h. Obviously, oxidative etching was greatly suppressed at low temperatures, and only truncated nanocubes were found in the products. On the contrary, when the reaction was conducted at a high temperature, the rate of etching was greatly enhanced, leading to the formation of 13 nm octahedra. In fact, changed in temperature can exponentially affect the reaction rate by varying the collision frequency between reactants as well as the number of activated molecules, leading to a significant change in the etching rate.[13] On the other hand, the reduction of newly formed Pd^{2+} ions was also dependent on oxidative etching. As a result, at 120 °C, $R_{etching}$ was very small whereas $R_{regrowth}$ was relatively large. In this case, octahedra of 23 nm in size should be the final products, but they could only be obtained at a much longer reaction time (results not shown). In contrast, at 140 °C, $R_{etching}$ would be substantially increased relative to $R_{regrowth}$, giving rise to the smallest octahedra with a size of 13 nm in a short period of time.

Finally, we examined the factors that can affect the oxidative etching process. To this end, another set of experiments was conducted. First, we note that the Pd nanocubes were very stable with a well-maintained cubic shape when they were heated in Tri-EG in the absence of HCl (Figure 4a). Even when NaCl was added, no noticeable change was observed over a time period of 2 h (Figure 4b). This observation again supported the results of many previous reports in which Cl^-/O_2 pairs were used to purify seeds with different crystallinity by selectively eliminating those with twin defects. Clearly, the Cl^-/O_2 pair alone could not work on the single-crystal Pd nanocubes.[7] When HCl was replaced with H_2SO_4, we did not observe significant etching of the Pd nanocubes either (Figure 4c), suggesting the critical role of Cl^- in accelerating the rate of etching. We then checked the function of O_2 from air. The experiment was carried out in droplet-based microreactors recently reported by many groups,[14] which could effectively prevent O_2 from entering into the reaction system (Figure S5). As shown in Figure 4d, we observed only slightly truncated nanocubes, demonstrating the crucial role played by O_2 in the etching process. Taken together, the etching reaction can be summarized as follows:

$$2Pd + O_2 + 8Cl^- + 4H^+ \rightarrow 2PdCl_4^{2-} + 2H_2O \quad (1)$$

Clearly, to complete the shape transformation from nanocubes to octahedra, Cl^-, H^+, and a trace amount of O_2 (from air) are all indispensible.

dx.doi.org/10.1021/ja406344j | J. Am. Chem. Soc. 2013, 135, 11752–11755

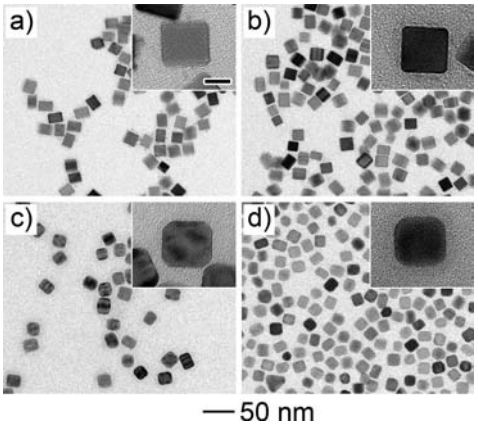

Figure 4. TEM images of Pd nanocrystals obtained using the standard etching process except for the following changes: (a) no etchant; (b) 60 μmol of NaCl instead of HCl; (c) 30 μmol of H_2SO_4 instead of HCl; (d) 60 μmol of HCl in droplet-based microreactors to avoid contact with O_2. The scale bar in the inset of (a) is 10 nm and applies to the other insets also.

In summary, Pd octahedra with different but controllable sizes were successfully prepared from Pd nanocubes with a single size. The synthesis was based upon an internal ripening process, as no additional Pd precursor was introduced. The success relied on the control of oxidative etching coupled with reduction of the newly formed Pd^{2+} ions for regrowth. Our results clearly show that the rates for etching and regrowth could be easily controlled simply by varying the concentration of HCl, allowing the formation of Pd octahedra with different sizes. We also demonstrated that O_2, Cl^-, and H^+ are all indispensible for the occurrence of oxidative etching of the single-crystal nanocubes. This work greatly advances our understanding of the role of oxidative etching in shape- and size-controlled synthesis of metal nanocrystals. We believe that this new strategy based upon etching and regrowth can also be extended to other metal nanocrystals.

■ ASSOCIATED CONTENT

Supporting Information

Experimental section and characterization details; calculation of the edge lengths of Pd octahedra derived from a cube; TEM images of nanocrystals obtained using a similar protocol except for smaller size or variation of the temperature. This material is available free of charge via the Internet at http://pubs.acs.org.

■ AUTHOR INFORMATION

Corresponding Author

younan.xia@bme.gatech.edu

Notes

The authors declare no competing financial interest.

■ ACKNOWLEDGMENTS

This work was supported in part by a grant from NSF (DMR-1215034), a DOE subcontract from the University of Wisconsin Madison (DE-FG02-05ER15731), and startup funds from Georgia Institute of Technology. As a visiting Ph.D. student from Xi'an Jiaotong University, M.L. was also partially supported by the China Scholarship Council (CSC).

■ REFERENCES

(1) (a) Nie, S.; Emory, S. R. *Science* **1997**, *275*, 1102. (b) Murphy, C. J.; Jana, N. R. *Adv. Mater.* **2002**, *14*, 80. (c) West, J. L.; Halas, N. J. *Annu. Rev. Biomed. Eng.* **2003**, *5*, 285. (d) Burda, C.; Chen, X.; Narayanan, R.; El-Sayed, M. A. *Chem. Rev.* **2005**, *105*, 1025. (e) Rosi, N. L.; Mirkin, C. A. *Chem. Rev.* **2005**, *105*, 1547. (f) Cozzoli, P. D.; Pellegrino, T.; Manna, L. *Chem. Soc. Rev.* **2006**, *35*, 1195. (g) Tao, A.; Sinsermsuksakul, P.; Yang, P. *Nat. Nanotechnol.* **2007**, *2*, 435. (h) Tian, N.; Zhou, Z.-Y.; Sun, S.-G.; Ding, Y.; Wang, Z. L. *Science* **2007**, *316*, 732. (i) Wang, C.; Daimon, H.; Onodera, T.; Koda, T.; Sun, S. *Angew. Chem., Int. Ed.* **2008**, *47*, 3588. (j) Xia, Y.; Xiong, Y.; Lim, B.; Skrabalak, S. E. *Angew. Chem., Int. Ed.* **2009**, *48*, 60. (k) McEachran, M.; Keogh, D.; Pietrobon, B.; Cathcart, N.; Gourevich, I.; Coombs, N.; Kitaev, V. *J. Am. Chem. Soc.* **2011**, *133*, 8066. (l) Zhang, H.; Jin, M.; Xia, Y. *Angew. Chem., Int. Ed.* **2012**, *51*, 7656.

(2) (a) Zhang, J.; Li, S.; Wu, J.; Schatz, G. C.; Mirkin, C. A. *Angew. Chem., Int. Ed.* **2009**, *48*, 7787. (b) Xia, Y.; Yang, P.; Sun, Y.; Wu, Y.; Mayers, B.; Gates, B.; Yin, Y.; Kim, F.; Yan, H. *Adv. Mater.* **2003**, *15*, 353. (c) Chen, S.; Carroll, D. L. *Nano Lett.* **2002**, *2*, 1003. (d) Lim, B.; Xiong, Y.; Xia, Y. *Angew. Chem., Int. Ed.* **2007**, *46*, 9279. (e) Cobley, C. M.; Rycenga, M.; Zhou, F.; Li, Z.-Y.; Xia, Y. *Angew. Chem., Int. Ed.* **2009**, *48*, 4824. (f) Rupich, S. M.; Shevchenko, E. V.; Bodnarchuk, M. I.; Lee, B.; Talapin, D. V. *J. Am. Chem. Soc.* **2010**, *132*, 289. (g) Huang, X.; Tang, S.; Zhang, H.; Zhou, Z.; Zheng, N. *J. Am. Chem. Soc.* **2009**, *131*, 13916. (h) Ahmadi, T. S.; Wang, Z. L.; Green, T. C.; Henglein, A.; El-Sayed, M. A. *Science* **1996**, *272*, 1924. (i) Chiu, C.-Y.; Li, Y.; Ruan, L.; Ye, X.; Murray, C. B.; Huang, Y. *Nat. Chem.* **2011**, *3*, 393.

(3) (a) Zhang, Q.; Hu, Y.; Guo, S.; Goebl, J.; Yin, Y. *Nano Lett.* **2010**, *10*, 5037. (b) Habas, S. E.; Lee, H.; Radmilovic, V.; Somorjai, G. A.; Yang, P. *Nat. Mater.* **2007**, *6*, 692. (c) Lim, B.; Jiang, M.; Camargo, P. H. C.; Cho, E. C.; Tao, J.; Lu, X.; Zhu, Y.; Xia, Y. *Science* **2009**, *324*, 1302. (d) Fan, F.-R.; Liu, D.-Y.; Wu, Y.-F.; Duan, S.; Xie, Z.-X.; Jiang, Z.-Y.; Tian, Z.-Q. *J. Am. Chem. Soc.* **2008**, *130*, 6949. (e) Seo, D.; Yoo, C. I.; Jung, J.; Song, H. *J. Am. Chem. Soc.* **2008**, *130*, 2940.

(4) (a) Xia, X.; Xie, S.; Liu, M.; Peng, H.-C.; Lu, N.; Wang, J.; Kim, M. J.; Xia, Y. *Proc. Natl. Acad. Sci. U.S.A.* **2013**, *110*, 6669. (b) Xie, S.; Lu, N.; Xie, Z.; Wang, J.; Kim, M. J.; Xia, Y. *Angew. Chem., Int. Ed.* **2012**, *51*, 10266.

(5) (a) Jin, M.; Zhang, H.; Xie, Z.; Xia, Y. *Energy Environ. Sci.* **2012**, *5*, 6352. (b) Wang, Y.; Wan, D.; Xie, S.; Xia, X.; Huang, C. Z.; Xia, Y. *ACS Nano* **2013**, *7*, 4586. (c) Xia, X.; Zeng, J.; Oetjen, L. K.; Li, Q.; Xia, Y. *J. Am. Chem. Soc.* **2012**, *134*, 1793.

(6) (a) Wiley, B.; Herricks, T.; Sun, Y.; Xia, Y. *Nano Lett.* **2004**, *4*, 1733. (b) Lim, B.; Jiang, M.; Tao, J.; Camargo, P. H. C.; Zhu, Y.; Xia, Y. *Adv. Funct. Mater.* **2009**, *19*, 189.

(7) (a) Wiley, B. J.; Xiong, Y.; Li, Z.-Y.; Yin, Y.; Xia, Y. *Nano Lett.* **2006**, *6*, 765. (b) Wiley, B. J.; Chen, Y.; McLellan, J. M.; Xiong, Y.; Li, Z.-Y.; Ginger, D.; Xia, Y. *Nano Lett.* **2007**, *7*, 1032. (c) Xiong, Y.; Chen, J.; Wiley, B.; Xia, Y.; Aloni, S.; Yin, Y. *J. Am. Chem. Soc.* **2005**, *127*, 7332.

(8) (a) Cobley, C. M.; Rycenga, M.; Zhou, F.; Li, Z.-Y.; Xia, Y. *J. Phys. Chem. C* **2009**, *113*, 16975. (b) Mulvihill, M. J.; Ling, X. Y.; Henzie, J.; Yang, P. *J. Am. Chem. Soc.* **2010**, *132*, 268.

(9) Zhang, T.; Ge, J.; Hu, Y.; Zhang, Q.; Aloni, S.; Yin, Y. *Angew. Chem., Int. Ed.* **2008**, *47*, 5806.

(10) Peng, H.-C.; Xie, S.; Park, J.; Xia, X.; Xia, Y. *J. Am. Chem. Soc.* **2013**, *135*, 3780.

(11) (a) Vitos, L.; Ruban, A. V.; Skriver, H. L.; Kollár, J. *Surf. Sci.* **1998**, *411*, 186. (b) Wang, Z. L. *J. Phys. Chem. B* **2000**, *104*, 1153.

(12) Jin, M.; Liu, H.; Zhang, H.; Xie, Z.; Liu, J.; Xia, Y. *Nano Res.* **2011**, *4*, 83.

(13) Connors, K. A. *Chemical Kinetics: The Study of Reaction Rates in Solution*; VCH: New York, 1990.

(14) (a) Song, H.; Chen, D. L.; Ismagilov, R. F. *Angew. Chem., Int. Ed.* **2006**, *45*, 7336. (b) Kim, Y. H.; Zhang, L.; Yu, T.; Jin, M.; Qin, D.; Xia, Y. *Small* **2013**, DOI: 10.1002/smll.201203132.